

sections from this inefficiency is smaller than the statistical errors on the points.

<sup>9</sup>C. W. Akerlof, P. K. Caldwell, C. T. Coffin, P. Kalbaci, D. I. Meyer, P. Schmueser, and K. C. Stanfield, *Phys. Rev. Lett.* **27**, 539 (1971).

<sup>10</sup>S. M. Pruss, C. W. Akerlof, D. I. Meyer, S. P. Ying, J. Lales, R. A. Lundy, D. R. Rust, C. E. W. Ward, and D. D. Yovanovitch, *Phys. Rev. Lett.* **23**, 189 (1969);

P. Kalbaci, C. W. Akerlof, P. K. Caldwell, C. T. Coffin, D. I. Meyer, P. Schmueser, and K. C. Stanfield, *Phys. Rev. Lett.* **27**, 74 (1971).

<sup>11</sup>A. Bashian, G. Finocchiaro, M. L. Good, P. D. Grannis, O. Guisan, J. Kirz, Y. Y. Lee, R. Pittman, G. C. Fischer, and D. D. Reeder, *Phys. Rev. D* **4**, 2667 (1971).

PHYSICAL REVIEW D

VOLUME 8, NUMBER 1

1 JULY 1973

### $K^+n$ Charge Exchange at 3.8 GeV/c\*

W. Moninger II,<sup>†</sup> B. Eisenstein, J. Kim, D. Marshall, T. A. O'Halloran, M. Robinson,<sup>‡</sup> and P. F. Schultz

*University of Illinois at Urbana-Champaign, Urbana, Illinois 61801*

(Received 3 August 1972)

We have found 431 events of the reaction  $K^+d \rightarrow K^0pp_s$  at 3.8-GeV/c  $K^+$  beam momentum in a 295 000-frame exposure of the Argonne National Laboratory 30-in. deuterium-filled bubble chamber. The event sample consists of one- and two-prong events with a visible  $K^0$  decaying to  $\pi^+\pi^-$ . The total and differential cross sections are found after correction for unseen  $K^0$ 's and for efficiencies in the scanning-measuring-fitting chain. Comparisons of the data are made to an SU(3) sum rule, a Regge model, and data for  $K^-p \rightarrow \bar{K}^0n$ .

#### I. INTRODUCTION

We present a study of the reaction

$$K^+n \rightarrow K^0p \quad (1)$$

at 3.8-GeV/c incident meson momentum. The data for our study consist of 431 examples of the reaction

$$K^+d \rightarrow K^0pp_s \quad (2)$$

from a 295 000-frame exposure of the Argonne National Laboratory (ANL) 30-in. deuterium-filled bubble chamber to the  $7^0$ -separated meson beam.

Our study consists of a determination of the total and differential cross section for reaction (1) and comparisons to (a) an SU(3) sum rule due to Barger and Cline<sup>1</sup> relating reaction (1) to the other three meson-nucleon  $I=1$  exchange reactions, (b) the predictions of a Regge model due to Rarita and Schwarzschild,<sup>2</sup> and (c) the total and differential cross-section data for the reaction

$$K^-p \rightarrow \bar{K}^0n. \quad (3)$$

A more detailed description of some aspects of this work is found in Ref. 3.

#### II. EXPERIMENTAL PROCEDURE

##### A. Scanning and Measuring

All one-prong-plus-vee events and all two-prong-plus-vee events with at least one positive stopping track from the primary vertex found in the scanning fiducial volume were measured on the Univer-

sity of Illinois SMP-CSX-1 system. Two thirds of the film was double-scanned, followed by a third scan to remove discrepancies between the two independent scans. The measurements were processed by the Illinois geometric reconstruction and kinematic fitting programs SPACE and ILLFIT. After the first measurement pass, those events that failed to be spatially reconstructed were measured again. Table I shows the final measurement disposition.

Line A of Table I gives the number of events that were measured and were not rejected either by a computer check of vertex location or by the measurers as being outside the fiducial volume. Line B gives the number of events that were reconstructed after any number of measurements (one, two, and in some special cases, three). Line C gives the estimated number of electron pairs in the sample. This correction was necessary because a study of a sample of events that failed to be reconstructed after repeated measurements revealed that many of these events had vees which were consistent with  $\gamma \rightarrow e^+e^-$  rather than  $K^0 \rightarrow \pi^+\pi^-$ . Such events could not be reconstructed by SPACE because of the zero-degree opening angle between the electrons. In some of these events, curvature and bubble density as observed on the scan table were consistent with decay electrons rather than pions. When extrapolated to the entire 9227 events measured,  $443 \pm 111$  or  $(4.8 \pm 1.2)\%$  are expected to contain electron-pair vees. Subtracting this number from the events that failed to be reconstructed gave the number of events that should have been reconstructed, but were not (line D in Table I). Assuming

TABLE I. Measurement disposition.

A. Events measured and inside fiducial volume:	9227
B. Events that were reconstructed inside fiducial volume:	7937
C. Estimated number of electron pairs [(4.8 ± 1.2)% of total]:	443 ± 111
D. Number of events that failed inside fiducial volume with electron pairs subtracted ( $a - b - c$ ):	847 ± 111
E. Scale factor for fitted events to give total number of events = $(a - c)/b$ :	1.11 ± 0.02

that final states occurred in the same proportions among the events that failed to be reconstructed (with electron pairs subtracted – line D in Table I) as in the events that were reconstructed (see below), the correction factor by which the number of events of each final state was scaled to account for the number lost due to measuring inefficiency was  $1.11 \pm 0.02$ . The error includes the statistical uncertainty in the number of events that fit (line B of Table I) as well as the error in the number of events that failed.

Evidence in support of the above assumption came from a comparison of the percentage of fits to reaction (2) found among (a) events that were reconstructed on the first measurement attempt, and (b) events that were reconstructed on a later attempt. The percentage was found to be the same within errors.

#### B. Fitting Procedures and Biases

All measured events were fitted to the hypothesis  $K^+d \rightarrow K^0pp_s$  (where  $p_s$  represents the spectator proton). In the one-prong events, the unfitted momentum of the unseen spectator was taken as  $p_x = p_y = 0 \pm 30$  MeV/c,  $p_z = 0 \pm 40$  MeV/c. The errors were chosen so that (a) the fitted momentum would correspond to an unseen spectator, provided that each component of the spectator momentum was within one standard deviation of the unfitted value, and (b) the fitted momentum distribution would be consistent with that predicted by the Hulthén wave function.<sup>4</sup>

The decay  $K^0 \rightarrow \pi^+ \pi^-$  was fitted first (3 constraints), and the fitted  $K^0$  was then used in a 4-constraint fit at the primary vertex. This yielded a net 7-constraint fit for the event. There were occasional failures of the fit to the  $K^0$  decay, primarily in events where the vee was far downstream, was steeply dipping, or for any other reason had decay tracks of short projected length. Failures were considered to be fits in which there was no convergence, or, in a few cases, in which the fitted  $\chi^2$  was so large that the 7-constraint fit failed to pass a 1%  $\chi^2$  probability cutoff. In case of such a failure, a 3-constraint fit was attempted for the primary vertex, using the  $K^0$  direction as given by the decay vertex.

All events with 7-constraint  $ppK^0$  fits which were ambiguous with any other hypothesis, and all events with 3-constraint  $ppK^0$  fits, were scanned by a physicist to check the consistency of the fit with bubble density and to verify that the event had been properly identified and measured. The final disposition of the fitting is shown in Table II.

*A priori*, we expect the 3c fits to be less reliable than the 7c fits. We expect the one-prong 3c fits to be contaminated to some extent by reactions such as



due to the large uncertainty in the spectator momentum combined with the unknown magnitude of the  $K^0$  momentum. (The fit is essentially unconstrained.) To check this possible bias, the missing mass recoiling off the protons was investigated.

Figure 1 presents the missing mass squared recoiling from the two protons. For the one-prong events, the mass was calculated assuming the spectator proton to be at rest. The figure is subdivided according to the resulting fit for each event: (a) 7c one-prong (1) and 7c two-prong (2) events, (b) 3c one-prong (1) and 3c two-prong (2) events, and (c) a sample of two-prong events giving fits to either reactions (2) or reaction (4). Figures 1(a2) and 1(b2) show that the two-prong 7c and 3c fits have a strong  $K^0$  signal, with very small background, if any.

The one-prong events, Figs. 1(a1) and 1(b1), on the other hand, show a very broad distribution around the  $K^0$  mass squared. This smearing out of the missing mass distribution for the one-prong

TABLE II.  $K^+d \rightarrow K^0pp_s$  fits with  $\chi^2$  probability  $P(\chi^2) > 1\%$ .

	Events
One-prong 7c fits	242
Two-prong 7c fits	161
One-prong 3c fits	(44) <sup>a</sup>
Two-prong 3c fits	28

<sup>a</sup>As indicated in the text, these events have not been included in any distributions.

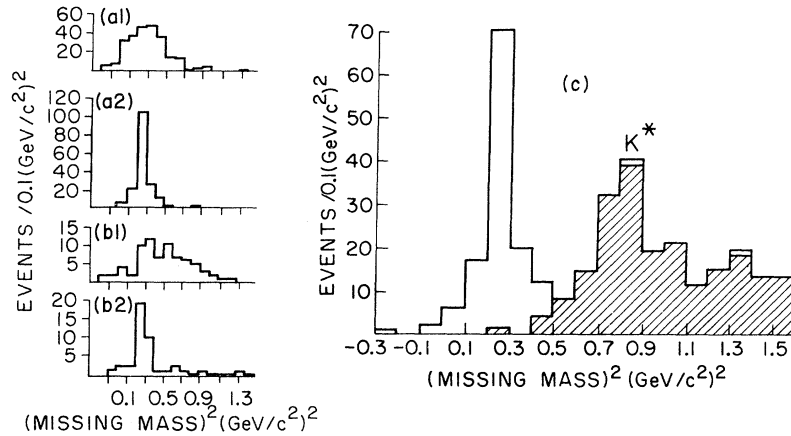


FIG. 1. Measured missing mass off the two protons for (a1) one-prong  $7c$   $ppK^0$  fits, (a2) two-prong  $7c$   $ppK^0$  fits, (b1) one-prong  $3c$   $ppK^0$  fits, (b2) two-prong  $3c$   $ppK^0$  fits, and (c) two-prong events fitting  $ppK^0$  or  $ppK^0\pi^0$  (shaded).

events is caused by the necessarily incorrect assignment of zero momentum for the unseen spectator. Nevertheless, the one-prong  $7c$  distribution 1(a1) shows, by its symmetry about the  $K^0$  mass squared, that these events are probably free of contamination due to reaction (4). The number of events above the  $K\pi$  threshold is entirely consistent with the tail of a broad Gaussian distribution centered on the value of the  $K^0$  mass squared. The one-prong  $3c$  distribution 1(b1) does not show this symmetry. The excess of events with high missing mass squared indicates probable contamination from reaction (4), as suggested by comparison to Fig. 1(c).

Because of this possible bias, the one-prong  $3c$ -fit events were removed from the final data sample, and the remaining  $3c$  and  $7c$  events were weighted to account for this loss. The remaining

events, both  $7c$  and  $3c$ , were required to have  $P(\chi^2)$  greater than 1% in order to be kept in the final data sample.

A study of 209  $7c$  fits that were measured and fitted twice, however, revealed that most of the events that fit reaction (2) with  $P(\chi)^2 < 1\%$  in one measurement fit reaction (2) with  $P(\chi)^2 > 1\%$  (and usually  $> 10\%$ ) in the other measurement. Thus, most of the fits with  $P(\chi)^2 < 1\%$  were judged to be examples of reaction (2) that were poorly measured. Therefore, the number of remaining events [with  $P(\chi)^2 > 1\%$ ] was scaled up by an appropriate factor (7%) for cross-section purposes.

### III. ANALYSIS AND RESULTS

#### A. Cross Sections

Table III gives a breakdown of the factors used to determine the total and differential cross sec-

TABLE III. Factors multiplying raw microbarn equivalent.

Scanning efficiency:	$0.935 \pm 0.018$
$K_S^0 \rightarrow (\text{neutrals})$ and $K_L^0$ :	$(2,911 \pm 0.02)^{-1}$
Odd prong $3c$ correction:	$(1.10 \pm 0.02)^{-1}$
Measuring efficiency:	$(1.11 \pm 0.02)^{-1}$
$P(\chi^2) < 1\%$ correction:	$(1.07 \pm 0.02)^{-1}$
Fitting efficiency:	$0.99 \pm 0.01$
Raw microbarn equivalent:	$0.183 \pm 0.004 \mu\text{b}/\text{ev}$
Corrected microbarn equivalent including above factors:	$0.753 \pm 0.033 \mu\text{b}/\text{ev}$
Number of $K^+d \rightarrow K^0 pp_s$ events (ev) found (from Table II; statistical error):	$431 \pm 21$
Number of events weighted for unseen $K_S^0 \rightarrow \pi^+ \pi^-$ and long spectators:	$661 \pm 32$
Cross section for these events:	$498 \pm 33 \mu\text{b}$

tions for reaction (2). The microbarn equivalent of this experiment was obtained by counting beam tracks entering every fiftieth frame. [Beam contamination was estimated to be negligible from a study of the beam profile ( $p$ ,  $K^+$ , and  $\pi^+$  peaks) just upstream of the final mass collimator, and from the Cherenkov counter monitor on the beam entering the chamber.] In addition to the corrections described in Sec. II and the recognition that  $K_L^0$  decays and  $K_S^0 \rightarrow$  (neutrals) events are not in our sample, we made the following corrections.

### 1. Unseen $K^0 \rightarrow \pi^+ \pi^-$ Correction

This correction was accomplished by weighting each event that was seen by the inverse of the probability that an event with such a vertex position,  $K^0$  direction, and momentum would actually have a visible and identifiable  $K^0$  decay. A  $K^0$  was assumed to have had a visible and identifiable decay if its length was greater than  $L_s = 0.25$  cm and less than  $L_l$ , the distance along the  $K^0$  direction to the edge of the "visible" region of the chamber.<sup>5</sup> The form of the weighting factor is

$$W = (e^{-L_s m / pc\tau} - e^{-L_l m / pc\tau})^{-1}, \quad (5)$$

where  $m$  is the mass of the  $K^0$ ,  $p$  is the laboratory momentum, and  $\tau$  is the  $K^0$  lifetime.

### 2. Fitting Efficiency

Not all  $K^+d \rightarrow K^0 p p_s$  events fit as such. We have already corrected for those that failed to reconstruct or fit any hypothesis in Sec. II. However, some reaction-(2) events may have fitted some other hypothesis and been lost from the reaction-(2) data sample. This effect was determined from remeasuring the good 7c and 3c events and fitting again. We found our fitting efficiency to be  $0.99 \pm 0.01$ .

### 3. Long Spectator Correction

As mentioned earlier, only events with spectators that stopped in the chamber were measured. We therefore had to correct for the loss of events in which the spectator escaped from the chamber. This was accomplished by comparing the spectator momentum distribution found in this experiment with the "true" distribution as found, for instance, in a  $\pi^+d$  exposure at 3.65 GeV/c due to Benson,<sup>6</sup> in which all spectators, both stopping and nonstopping, were measured. We used 1916 four-prong fitted events from our exposure to compare with Benson's distribution. We used the momentum range 110–250 MeV/c (real length 0.4–0.8 cm) to normalize Benson's data to our sample. 902 events with spectator momentum above 250 MeV/c were predicted for our sample, whereas we had only 194

events. The correction factor for our two-prong events is, therefore,  $R = 1.37 \pm 0.05$ .

The cross section for reaction (2) using the factors listed in Table III is then

$$\sigma(K^+d \rightarrow K^0 p p_s) = 498 \pm 33 \text{ } \mu\text{b}. \quad (6)$$

To obtain the cross section for the charge-exchange reaction (1), two corrections for effects due to the deuteron target were necessary: (a) a correction for the depletion of events due to one nucleon of the deuteron "shadowing" the other (Glauber screening),<sup>7</sup> and (b) a correction for the effect of the Pauli exclusion principle operating on the two final-state protons to decrease the number of events near the forward direction.

A small correction must be made to account for Glauber screening in the deuteron. We assume that partial cross sections off single nucleons in deuterium are in the same ratio to the cross sections off free nucleons as is  $\sigma_T(K^+n) + \sigma_T(K^+p)$  to  $\sigma_T(K^+d)$ . At our energy, this implies an increase in differential and total cross sections by the factor 1.016.

The Pauli correction was  $t$ -dependent, and quite large and uncertain for the low- $|t|$  events. We made the correction using a form<sup>8</sup>

$$\left(\frac{d\sigma}{dt}\right)_n = \left(\frac{d\sigma}{dt}\right)_a \frac{1+R}{1-H+R(1-H/3)}, \quad (7)$$

where  $H$  is the deuteron form factor, and  $R$  is the ratio of the spin-flip contribution to the differential cross section to the spin-nonflip contribution.

The uncertainty in this correction comes partly from the unknown ratio,  $R$ . We took  $R(t) = R(0) = 0$  because the spin-flip amplitude must vanish at  $t=0$  due to kinematics. At higher  $|t|$ , where this approximation is in error, the correction is slight anyway.

A large uncertainty in the correction comes from the strong  $t$  dependence of  $H$  at low  $|t|$ . Although  $H(t)$  is reasonably well known, the fractional error in  $|t|$  is large in the low- $|t|$  events. A small absolute error in  $|t|$  on any given event may cause a large error in the Pauli correction.

The differential cross section for reaction (2) is tabulated in Table IV and plotted in Fig. 2. The errors on the corrected points representing reaction (1) include the uncertainty in the value of (7) because of the error on  $t$  as well as the statistical error.

Using a smooth eyeball fit (not shown) to the corrected points in Fig. 2, we find a total charge-exchange cross section of

$$\sigma(K^+n \rightarrow K^0 p) = 566 \pm 41 \text{ } \mu\text{b}. \quad (8)$$

For momentum transfers above  $|t| = 0.15$

TABLE IV. Differential cross section for  $K^+d \rightarrow K^0pp_s$ .

$-t$ [(GeV/c) <sup>2</sup> ]	$\frac{d\sigma}{dt}$ [ $\mu\text{b}/(\text{GeV}/c)^2$ ]
0-0.05	701 ± 132
0.05-0.10	790 ± 136
0.10-0.15	967 ± 164
0.15-0.20	1473 ± 200
0.20-0.25	1045 ± 156
0.25-0.30	820 ± 146
0.30-0.35	666 ± 124
0.35-0.45	475 ± 75
0.45-0.55	334 ± 67
0.55-0.70	224 ± 44
0.70-0.85	93 ± 27
0.85-1.10	59 ± 17

(GeV/c)<sup>2</sup>, the data fit well to the form  $d\sigma/dt = Ae^{bt}$ , where  $A = 2760 \pm 370 \mu\text{b}/(\text{GeV}/c)^2$  and  $b = 4.1 \pm 0.3 (\text{GeV}/c)^{-2}$ .

From the differential cross section, we can infer the phase of the forward scattering amplitude as follows: From Fig. 2 and our eyeball fit, we estimate that  $d\sigma/dt|_{t=0} = 1800 \pm 700 \mu\text{b}/(\text{GeV}/c)^2$ . If the amplitude were purely imaginary at  $t=0$ , then the optical theorem would read

$$\left. \frac{d\sigma}{dt} \right|_{t=0} = [\sigma_T(K^+n) - \sigma_T(K^+p)]^2 / 16\pi.$$

Using  $\sigma_T(K^+p) = 17.14 \pm 0.174 \text{ mb}$  at 3.3 GeV/c, and  $\sigma_T(K^+n) = 17.55 \pm 0.182 \text{ mb}$  at 3.3 GeV/c,<sup>9</sup> yields  $d\sigma/dt|_{t=0} = 8.6 \pm 10.6 \mu\text{b}/(\text{GeV}/c)^2$ . Comparison of this value with our estimated value gives

$$\left. \frac{\text{Im}(f)}{\text{Re}(f)} \right|_{t=0} \leq (6.9 \pm 7.8)\%.$$

#### IV. COMPARISONS

Figure 2 compares our data to the prediction of an SU(3) sum rule due to Barger and Cline<sup>1</sup>:

$$\begin{aligned} \frac{d\sigma}{dt}(K^+n \rightarrow K^0p) &= \frac{d\sigma}{dt}(\pi^-p \rightarrow \pi^0n) + 3 \frac{d\sigma}{dt}(\pi^-p \rightarrow \eta n) \\ &\quad - \frac{d\sigma}{dt}(K^-p \rightarrow K^0n). \end{aligned} \quad (9)$$

(A similar relationship obtains for total cross sections.)

Data<sup>10-12</sup> on the three reactions listed on the right-hand side of Eq. (9) have been extrapolated to  $p_{\text{lab}} = 3.8 \text{ GeV}/c$  using the parametrization  $\sigma \sim (p_{\text{lab}})^{-n}$ . The value of  $n$  was estimated from published cross-section data on each reaction, and gave an extrapolation of, at most, 15% in the cross sections used for the test.

Although our data agree with the sum-rule prediction for the shape of  $d\sigma/dt$ , they are much

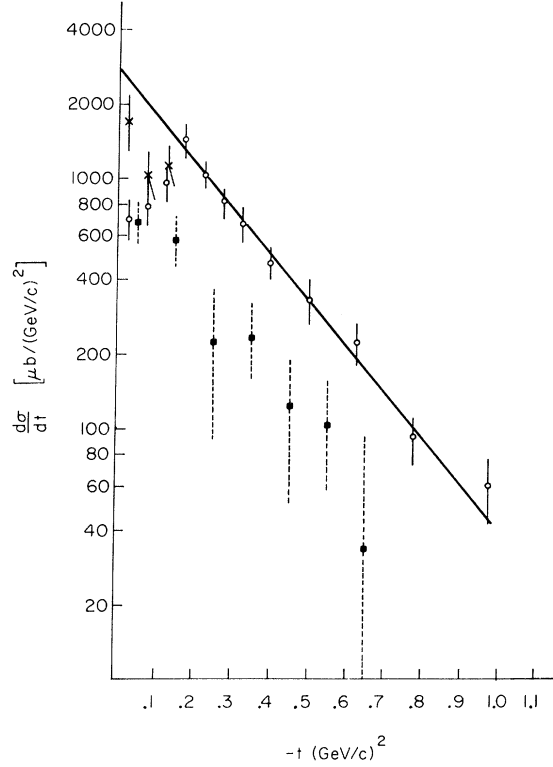


FIG. 2. Differential cross section for  $K^+d \rightarrow K^0pp$  (open circles). Not shown is the contribution from 32 events with  $|t| > 1.1 (\text{GeV}/c)^2$ . The differential cross section for  $K^+n \rightarrow K^0p$  resulting from the deuteron correction is indicated by the crosses where the correction is significant. The solid line is the exponential fit to the data for  $|t| > 0.15 (\text{GeV}/c)^2$ . The prediction of the SU(3) sum rule for  $d\sigma/dt(K^+n \rightarrow K^0p)$  is shown by the squares.

larger in magnitude (see Fig. 2). This is emphasized by the sum-rule prediction for the total charge-exchange cross section,  $\sigma_{\text{SU}(3)}(K^+n \rightarrow K^0p) = 222 \pm 41 \mu\text{b}$ , which must be compared to our value (8).

Figure 3 shows our data compared to a Regge-model prediction due to Rarita and Schwarzschild.<sup>2</sup> They assumed the exchange of a  $\rho$ ,  $A_2$ , and a hypothetical  $\rho'$  trajectory having  $\alpha(0)$  one unit below the  $\rho$  and the same  $C$  parity as the  $\rho$ . Although this model relies rather heavily on the  $\rho'$ , a trajectory whose existence is currently unclear, it has been a rather successful parametrization for fitting  $K^+d$  (Ref. 13) and  $K^-p$  (Ref. 14) charge-exchange reactions through the region  $p_{\text{lab}} = 2.3-12 \text{ GeV}/c$ . Figure 3 shows the prediction of the model compared with our data. Although we get  $\chi^2 = 38$  for 12 data points, the fit appears to be adequate, at least in the shape of  $d\sigma/dt$ .

Figure 4 shows the effective trajectory for reaction (2), defined by

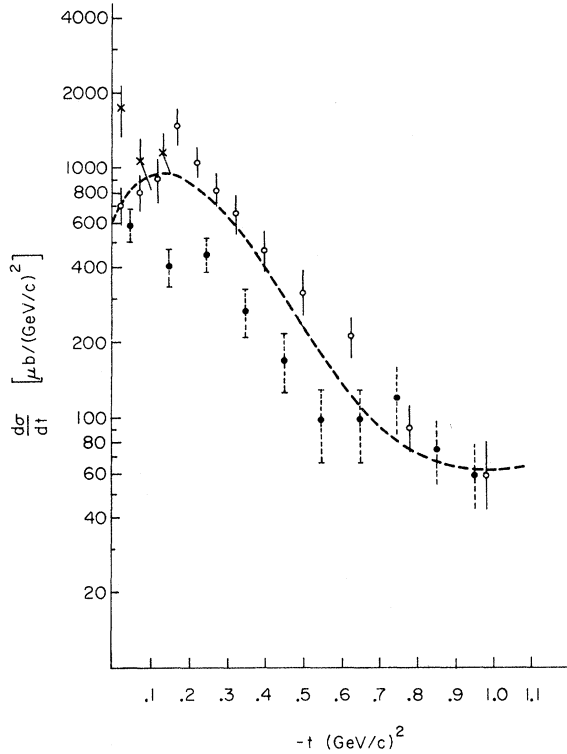


FIG. 3. Open circles and crosses as in Fig. 2. The dashed curve is the prediction at 3.8 GeV/c of the Regge model and fitted parameters of Ref. 3. The solid circles are the differential cross section for  $K^-p \rightarrow K^0n$  at 3.9 GeV/c (Ref. 12).

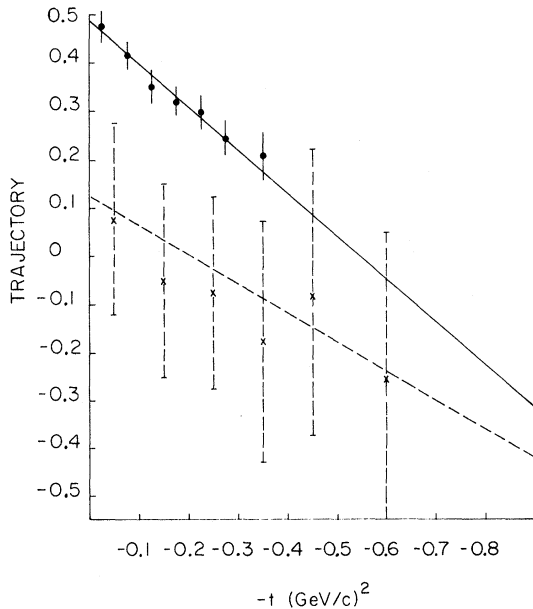


FIG. 4. Effective Regge trajectories for  $\pi^-p \rightarrow \pi^0n$  (solid line) and  $K^+n \rightarrow K^0p$  (dashed line).

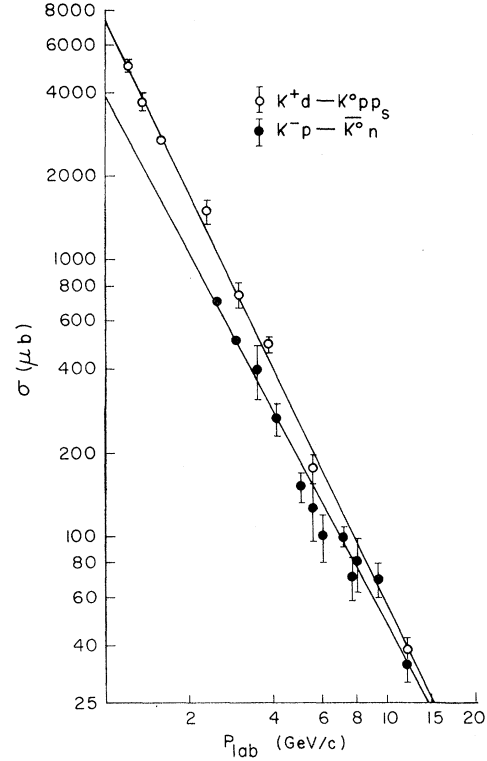


FIG. 5. Comparison of  $K^+d$  (open circles) and  $K^-p$  (solid circles) charge-exchange cross sections. The straight lines are fits described in the text.

$$\frac{d\sigma}{dt}(K^+d \rightarrow K^0pp_s) \sim F(t)p_{\text{lab}}^{2\alpha_{\text{eff}}(t)-2}.$$

The form of  $\alpha_{\text{eff}}$  has been determined using only the data at higher momenta: 3.8 GeV/c (this experiment), 5.5 GeV/c (Ref. 15), and 12 GeV/c (Ref. 16). The resulting fit yields

$$\alpha_{\text{eff}}(t) = (0.12 \pm 0.20) + (0.6 \pm 0.5)t. \quad (10)$$

For comparison, data on  $\pi^+p \rightarrow \pi^0n$  (Ref. 17) are also shown in Fig. 4. These data yield

$$\alpha_{\text{eff}}(\pi^+p \rightarrow \pi^0n) = (0.48 \pm 0.03) + (0.87 \pm 0.10)t,$$

which is consistent with the  $\rho$  or  $A_2$ .

Figure 5 presents  $K^+d$  and  $K^-p$  charge-exchange total cross-section data for incident momenta above 1.19 GeV/c for the  $K^+$  reaction, and above 2.49 GeV/c for the  $K^-$  reaction. For clarity, we have not plotted  $K^-p$  data points between 2.49 and 3 GeV/c. Although the  $K^+d$  cross sections are within errors, consistent with the  $K^-p$  results at 5.5 and 12 GeV/c, the data also fit functions of the form  $\sigma = A p_{\text{lab}}^{-n}$ . The straight lines in Fig. 5 are the best fits to this form, being

$$\sigma(K^+d \rightarrow K^0pp_s) = (7300 \pm 260)p_{\text{lab}}^{-2.09 \pm 0.04} \mu\text{b}, \quad (11)$$

$$\sigma(K^-p \rightarrow K^0n) = (3740 \pm 160)p_{\text{lab}}^{-1.87 \pm 0.04} \mu\text{b}. \quad (12)$$

The fit in Eq. (11) has a  $\chi^2$  of 8.4 for 8 data points, and in Eq. (12) a  $\chi^2$  of 32 for 22 data points. To avoid possible low-energy effects in  $K^-p$  charge exchange, another fit was made to the data above 3.4 GeV/c, and an exponent of  $-1.74 \pm 0.02$  resulted.

Regge models with degenerate  $\rho$  and  $A_2$  trajectories  $\alpha_\rho(t) = \alpha_{A_2}(t)$  naturally lead to the prediction of equality of both the differential and total cross sections for  $K^+$  and  $K^-$  nucleon charge-exchange scattering. The  $K^+n$  data at 5.5 and 12 GeV/c agree with this prediction and have been interpreted as strong evidence for simple ( $\rho, A_2$ ) degeneracy. However, were the cross-section dependence to continue the trend of the straight lines in Fig. 5 at higher energy, the prediction would be violated. It is significant to note that at 3.8 GeV/c our  $K^+n$  differential cross section agrees in shape with the  $K^-p$  data at 3.9 GeV/c,<sup>12</sup> although it is much larger in magnitude (see Fig. 3). Moreover, if we assume, in standard Regge fashion, that  $\sigma \sim p_{\text{lab}}^{2\alpha(0)-2}$ , the exponents from our fits imply

$\alpha(0) \sim 0$ , in agreement with (10), rather than  $\alpha_\rho(0) \approx \alpha_{A_2}(0) \approx \frac{1}{2}$ .

Data at higher energy could establish whether the form  $\sigma = A p_{\text{lab}}^{-n}$  persists, while the  $K^+$  and  $K^-$  differential cross sections maintain the same shape. On the other hand, new data in the region above 4-GeV/c  $K^+$  momentum might reveal that  $\sigma_{K^+}$  does, indeed, approach  $\sigma_{K^-}$ .

#### ACKNOWLEDGMENTS

The authors wish to acknowledge the kind assistance of Dr. H. Gordon and Jo Ann Kazenski. We also wish to thank the crew of the MURA 30-in. bubble chamber at ANL for their help during the experimental run, the University of Illinois' scanning and measuring staff under the direction of Mary Jo Pelafas, and the computer staff under the direction of Nancy Czechowski, for their help with the analysis.

\*Work supported in part by the U.S. Atomic Energy Commission.

†Present address: Coe College, Cedar Rapids, Iowa 52402

‡Present address: Physics Department, University of Wisconsin, Madison, Wisconsin 53706

<sup>1</sup>V. Barger and D. Cline, *Phys. Rev.* **156**, 1522 (1967).

<sup>2</sup>W. Rarita and B. M. Schwarzschild, *Phys. Rev.* **162**, 1378 (1968).

<sup>3</sup>W. R. Moninger, Ph.D. thesis, University of Illinois, 1971 (unpublished).

<sup>4</sup>M. Moravcsik, *Nucl. Phys.* **7**, 113 (1958).

<sup>5</sup>Limits to the visible region of the chamber were 1 cm inside the glass faces, and a cylinder of radius 29 cm centered in the chamber.

<sup>6</sup>G. C. Benson, Ph.D. thesis, University of Michigan, 1966 (unpublished).

<sup>7</sup>R. J. Glauber, *Phys. Rev.* **100**, 242 (1955).

<sup>8</sup>W. Lee, Ph.D. thesis, University of California, 1961 (unpublished).

<sup>9</sup>L. R. Price, N. Barash-Schmidt, O. Benary, R. W. Bland, A. H. Rosenfeld, and C. G. Wohl, LBL Report No. UCRL 20000  $K^+N$ , 1969 (unpublished). The  $K^+n$  and  $K^-p$  total cross sections vary slowly between 3 and 4 GeV/c, so we may use these data for the comparison.

<sup>10</sup>M. A. Wahlig and I. Mannelli, *Phys. Rev.* **168**, 1515 (1968).

<sup>11</sup>O. Guisan, J. Kirz, P. Sonderegger, A. V. Stirling, P. Borgeaud, C. Bruneton, F. Falk-Vairant, B. Amblard, C. Caversasio, J. P. Guillaud, and M. Yvert, *Phys. Lett.* **18**, 200 (1965).

<sup>12</sup>M. Aguilar-Benitez, R. L. Eisner, and J. B. Kinson, *Phys. Rev. D* **4**, 2583 (1971).

<sup>13</sup>A. A. Hirata, C. G. Wohl, G. Goldhaber, and G. H. Trilling, *Phys. Rev. Lett.* **21**, 1485 (1968); I. Butterworth, J. L. Brown, G. Goldhaber, S. Goldhaber, A. A. Hirata, J. A. Kadyk, B. M. Schwarzschild, and G. H. Trilling, *ibid.* **15**, 734 (1965). Y. Goldschmidt-Clermont, V. P. Henri, B. Jongejans, U. Kundt, F. Muller, R. L. Sekulin, M. Shafi, G. Wolf, J. M. Crispeels, J. Debaisieux, M. Delabaye, P. Dufour, F. Grard, J. Heughebaert, J. Naisse, G. Thill, R. Windmolders, K. Buchner, G. Dehm, G. Goebel, H. Hupe, T. Joldersma, I. S. Mitra, and W. Wittek, *Phys. Lett.* **27B**, 602 (1968); D. Cline, J. Penn, and D. D. Reeder, University of Wisconsin Report No. COO-881-258 (unpublished); D. Cline, J. Matos, and D. D. Reeder, *Phys. Rev. Lett.* **23**, 1318 (1969); A. Firestone, G. Goldhaber, A. Hirata, D. Lissauer, and G. H. Trilling, *ibid.* **25**, 958 (1970).

<sup>14</sup>C. Bricman, M. Ferro-Luzzi, J.-M. Perreau, G. Bizard, Y. Déclais, J. Duchon, J. Seguinot, and G. Valladas, *Phys. Lett.* **31B**, 148 (1970); G. W. London, R. R. Rau, N. P. Samios, S. S. Yamamoto, M. Goldberg, S. Lichtman, M. Prime, and J. Leitner, *Phys. Rev.* **143**, 1034 (1966); A. D. Brody and L. Lyons, *Nuovo Cimento* **45A**, 1027 (1966); P. Astbury, G. Brautti, G. Finocchiaro, A. Michelini, K. Terwilliger, D. Websdale, C. H. West, P. Zanella, W. Beusch, W. Fischer, B. Gobbi, M. Pepin, and E. Polgar, *Phys. Lett.* **23**, 396 (1966); A. Buffington, D. H. Frisch, and C. E. W. Ward, *Phys. Rev.* **176**, 1228 (1969).

<sup>15</sup>See Cline, Matos, and Reeder (Ref. 13).

<sup>16</sup>See Firestone *et al.* (Ref. 13).

<sup>17</sup>G. Giacomelli, P. Pini, and S. Stagni, CERN Report No. CERN/HERA 69-1 (unpublished).